Dalton Transactions

Cite this: *Dalton Trans.*, 2011, **40**, 2787

www.rsc.org/dalton

PAPER

$^{99m}Tc(CO)_3$-labeled pamidronate and alendronate for bone imaging†

Elisa Palma, João D. G. Correia, Bruno L. Oliveira, Lurdes Gano, Isabel C. Santos and Isabel Santos*

Received 15th October 2010, Accepted 15th December 2010
DOI: 10.1039/c0dt01396j

Bone scintigraphy with ^{99m}Technetium-methylenediphosphonate (^{99m}Tc-MDP) or ^{99m}Technetium-hydroxymethylenediphosphonate (^{99m}Tc-HMDP) presents several limitations, namely low specificity, uncertainty in the radiopharmaceutical's molecular structure and long acquisition time after injection. Aiming to find bone-seeking radiotracers based on the core *fac*-$[^{99m}Tc(CO)_3]^+$ with improved chemical and biological properties, we synthesized new conjugates (pz-PAM and pz-ALN), comprising a pyrazolyl-diamine chelating unit (pz: *N*,*N*,*N* donor atom set) for metal stabilization and a pendant pamidronate (PAM) or alendronate (ALN) moiety for bone targeting. The reaction of the conjugates with *fac*-$[^{99m}Tc(CO)_3]^+$ yielded (> 95%) the stable complexes *fac*-$[^{99m}Tc(CO)_3$(pz-PAM)$]^-$ (**2a**) and *fac*-$[^{99m}Tc(CO)_3$(pz-ALN)$]^-$ (**3a**), which have been characterized by comparing their HPLC gamma-traces with the UV-vis traces of the Re surrogates **2** and **3**, respectively. **2a** and **3a** bind strongly onto hydroxyapatite. The biodistribution studies in Balb-c mice have shown that **2a** and **3a** presented an high bone uptake (**2a** 18.3 ± 0.6% I.D./g, **3a** 17.3 ± 6.1% I.D./g, at 1 h post injection), similar to ^{99m}Tc-MDP (17.1 ± 2.4% I.D./g, at 1 h post injection), with comparable clearance from most tissues and increased total excretion (**2a** 66% I.D., **3a** 67% I.D. and ^{99m}Tc-MDP 49% I.D., at 1 h post injection). The bone-to-blood (**2a** 86.2, **3a** 74.7) and the bone-to-muscle ratios (**2a** 77.7, **3a** 79.0) are higher than the ones found for ^{99m}Tc-MDP (70.9, 47.9), at 4 h post injection. Planar whole-body gamma camera images of the rats injected with the $^{99m}Tc(CO)_3$-labeled pamidronate (**2a**) and alendronate (**3a**) confirmed the overall adequate biological profile of the new radiotracers for bone imaging.

Introduction

1,1-bisphosphonates (BPs) present a very high affinity for the bone mineral matrix, binding strongly to the hydroxyapatite (HA) crystals, which are its main component. BPs such as pamidronate and alendronate are preferentially incorporated into the sites of intense metabolic activity in bone, being indicated in the treatment of Paget's disease, osteoporosis and malignancies metastatic to bone.[1,2] ^{99m}Technetium-methylenediphosphonate (^{99m}Tc-MDP) and ^{99m}Technetium-hydroxymethylenediphosphonate (^{99m}Tc-HMDP) are the SPECT radiopharmaceuticals of choice for skeletal imaging, being widely used for the assessment of bone metastases, especially in breast and prostate cancer.[3,4] The therapeutic "analog" ^{186}Rhenium-hydroxyethylidene-1,1-diphosphonate (^{186}Re-HEDP) is used for metastatic bone pain palliation.[5–7] In spite of their well established use in nuclear medicine as diagnostic or therapeutic agents, ^{99m}Tc- and ^{186}Re-labelled BPs present a set of recognized clinical and physicochemical limitations. From a clinical point of view, the ^{99m}Tc-BPs may lead to false negatives due to the lack of specificity in certain disease states. These radiopharmaceuticals exist as a mixture of polymeric charged compounds, with unknown structure and varying properties along time, being rapidly degraded *in vivo* (oxidation to $[^{99m}TcO_4]^-$ or $[ReO_4]^-$).[8] Moreover, ^{99m}Tc-BPs display a relatively slow blood and soft-tissue clearance, delaying the start of the bone-scanning procedure in nuclear medicine centres. Taken together, the above mentioned drawbacks prompted several research efforts towards the development of novel ^{99m}Tc- and ^{186}/^{188}Re-labelled BPs for bone imaging and therapy, respectively.[9–22] The most successful strategies have used the bifunctional chelating approach. In this approach, the affinity for the bone is expected to be increased compared to ^{99m}Tc-MDP and ^{99m}Tc-HMDP, since the BP group does not coordinate to the metal, retaining its full ability for binding to the bone surface. Verbeke *et al.* have used the ^{99m}Tc(V) oxocomplex ^{99m}Tc-ethylene dicysteine (^{99m}Tc-EC) covalently bound to aminomethylenediphosphonate (^{99m}Tc-EC-AMDP) to obtain scintigraphic images in a baboon, showing good quality bone scans.[11] Ogawa *et al.* introduced a ^{99m}Tc-mercaptoacetylglycylglycylglycine (MAG_3)-conjugated hydroxy-bisphosphonate (^{99m}Tc-MAG_3-HBP, HBP = alendronate) and a ^{99m}Tc-6-hydrazinopyridine-3-carboxylic acid (HYNIC)-conjugated hydroxy-bisphosphonate (^{99m}Tc-HYNIC-HBP).[12] The complexes had higher affinity for hydroxyapatite and a higher *in vivo* bone uptake than ^{99m}Tc-HMDP. However, despite its unknown structure, ^{99m}Tc-HYNIC-HBP was revealed to be the

Unidade de Ciências Químicas e Radiofarmacêuticas, ITN, Estrada Nacional 10, 2686-953 Sacavém, Portugal. E-mail: isantos@itn.pt

† Electronic supplementary information (ESI) available. CCDC reference number 789827. See DOI: 10.1039/c0dt01396j

most promising for bone scintigraphy, since it displayed the highest bone-to-blood ratio.[12] The remarkable chemical features shown by the low-oxidation core *fac*-$[M(CO)_3]^+$ (M = ^{99m}Tc, Re) prompted us to synthesize and evaluate the well defined $^{99m}Tc(CO)_3$-complex **1a** as bone-seeking agent.[13,23–25] Complex **1a** displayed an adequate *in vivo* pharmacokinetic profile for bone targeting, namely favourable bone-to-blood and bone-to-muscle ratios (Fig. 1).[13] Additionally, it presented also excellent *in vivo* stability, confirming the high ability of pyrazolyl-diamine type chelators to stabilize the *fac*-$[^{99m}Tc(CO)_3]^+$ core and to label bisphosphonates using the bifunctional approach.[13,25]

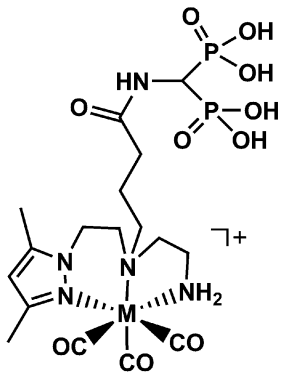

M = Re (**1**), ^{99m}Tc (**1a**)

Fig. 1 M(I) complexes **1**/**1a** containing a pendant aminomethylenediphosphonic acid group.[13]

Aiming to improve the bone-seeking properties of **1a**, we report herein the synthesis and characterization of analog complexes bearing pamidronate and alendronate (**2**/**2a** and **3**/**3a**, Fig. 2) as bone-seeking moieties. The *in vivo* biodistribution studies of **2a** and **3a** in Balb-c mice and imaging of Sprague Dawley rats are described. While this work was in progress, de Rosales *et al.*, using a similar synthetic approach, reported a promising tricarbonyl complex for bone imaging anchored on a pyridine derivative and bearing alendronate as the targeting vector ($^{99m}Tc(CO)_3$-DPA-BP, DPA = dipicolylamamine, BP = alendronate).[9]

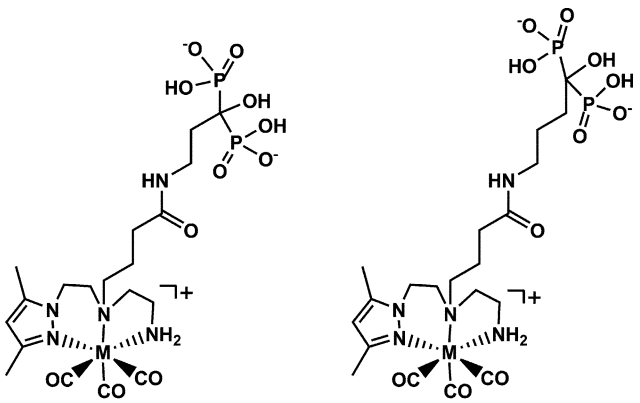

M = Re (**2**), ^{99m}Tc (**2a**) M = Re (**3**), ^{99m}Tc (**3a**)

Fig. 2 Re- and ^{99m}Tc-tricarbonyl complexes **2**/**2a** and **3**/**3a** containing pendant pamidronate and alendronate units, respectively.

Results and discussion

Synthesis and characterization of pz-PAM and Pz-ALN

The bisphosphonate-containing bioconjugates pz-PAM (PAM: pamidronate) and Pz-ALN (ALN: alendronate) were prepared as depicted in Scheme 1.

The bioconjugate pz-PAM has been synthesized in a two-step procedure, starting with the activation of the free carboxylic acid group of the precursor pz(Boc)–COOH with *N*-hydroxysuccinimide/DCC, followed by reaction with pamidronate in a mixture of CH_3CN/borate buffer pH 9.5 and triethylamine. Pz-ALN was obtained in a one pot reaction by direct conjugation of the precursor pz(Boc)–COOH with alendronate, using HOBt/HBTU and 4-methylmorpholine (NMM) in a DMF–H_2O mixture. For both compounds, the final step involved Boc-deprotection, followed by purification. The bioconjugates pz-PAM and pz-ALN have been obtained with a high chemical purity (> 98%) and were characterized by multinuclear NMR (^{1}H, ^{13}C and ^{31}P), and IR spectroscopy, electrospray ionization mass spectrometry (ESI-MS) and elemental analysis. The use of 2D-NMR experiments was crucial for the NMR assignment.

fac-$[Re(CO)_3$(pz-PAM)$]^-$ (2) and *fac*-$[Re(CO)_3$(pz-ALN)$]^-$ (3): synthesis and characterization

The Re(I)-complexes *fac*-$[Re(CO)_3$(pz-PAM)$]^-$ (**2**) and *fac*-$[Re(CO)_3$(pz-ALN)$]^-$ (**3**) were prepared and fully characterized as non radioactive surrogates of the corresponding ^{99m}Tc(I)-complexes **2a** and **3a** (Scheme 2).

Complexes **2** and **3** were synthesized by reacting the previously described rhenium precursor *fac*-$[Re(CO)_3(k^3$-pz-COOH$)]^+$ with the corresponding bisphosphonate (see experimental section).[13,26] An ORTEP diagram of *fac*-$[Re(CO)_3(k^3$-pz-COOH$)]^+$ is depicted in Fig. 3.

In this rhenium tricarbonyl precursor, the metal centre is six-coordinated, with one of the triangular faces of the octahedron defined by three carbonyl ligands and the other by the nitrogen atoms of the pyrazolyl ligand. The Re–C and Re–N bond distances and angles can be considered to be unexceptional and are in the range found for other tricarbonyl complexes stabilized by the same type of ligands.[13,25,26]

Complexes **2** and **3** were characterized by multinuclear NMR (^{1}H, ^{13}C and ^{31}P) and IR spectroscopy, ESI-MS and elemental analysis. The ^{1}H-NMR spectra of **2** and **3** displayed sharp singlet peaks assigned to the H (4) (δ 6.07, **2**; 6.02, **3**) and methyl groups (δ 2.30/2.19, **2**; δ 2.26/2.18, **3**) of the azolyl ring. Moreover, the chemical shifts and splitting pattern of the diastereotopic amine protons (δ 5.06–5.11 and δ 3.64) and the methylenic protons of the coordinating conjugates pz-PAM and pz-ALN are comparable to those found for similar compounds that were previously described.[13,25,26] Based on the pattern of the NMR spectra, it is clear that pz-PAM and pz-ALN coordinate to the metal as neutral and tridentate ligands, through the nitrogen atoms of the pyrazolyl-diamine ligand backbone (*N*,*N*,*N* donor-atom set).

The ^{13}C spectra showed 19 and 20 peaks, which correspond to all the carbon nuclei expected for **2** and **3**, respectively. The ^{31}P NMR spectra in D_2O presented only one singlet at δ 24.7 and δ 19.6 for **2** and **3**, respectively. These resonances are slightly

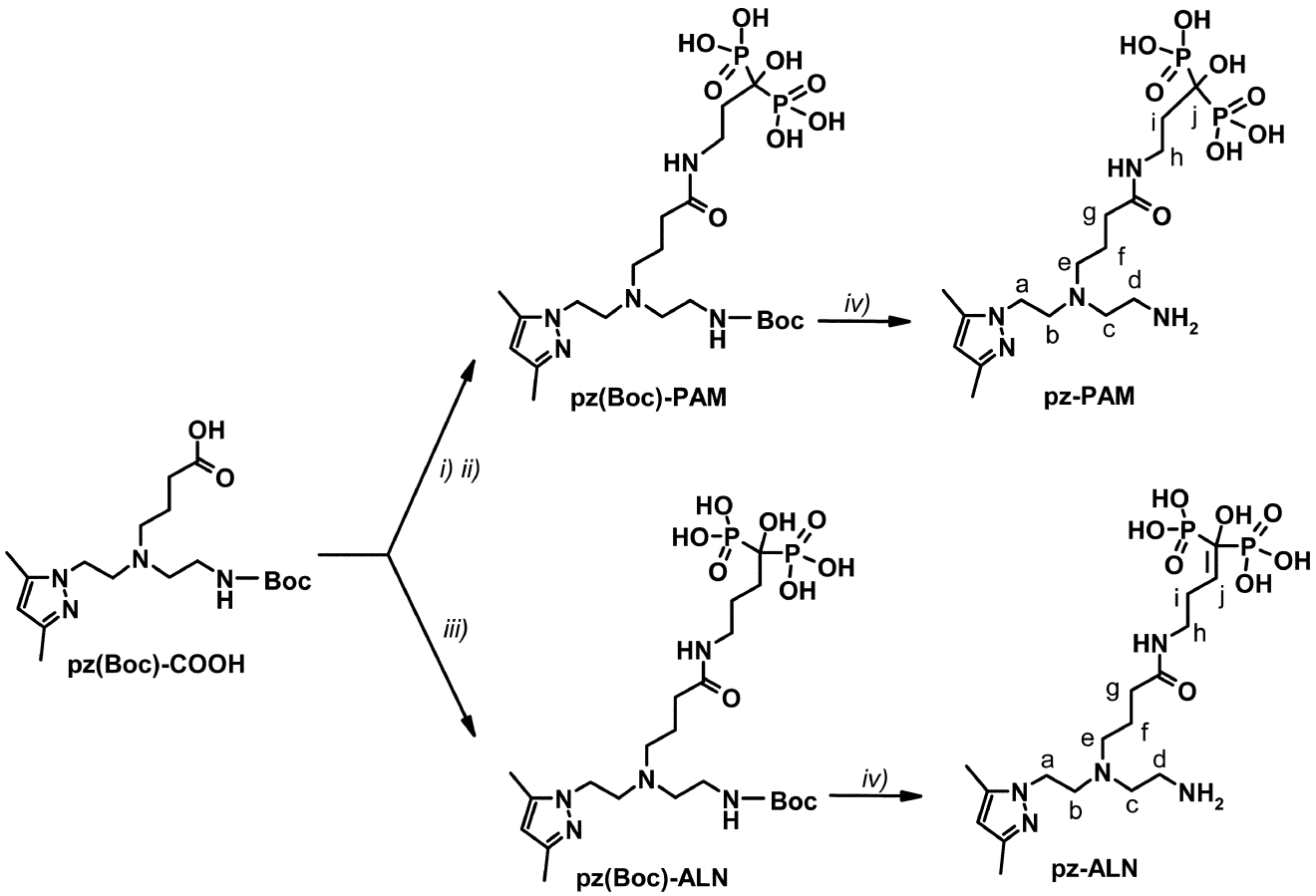

Scheme 1 The synthesis of the bisphosphonate-containing conjugates pz-PAM and pz-ALN. (i) NHS/DCC, CH_2Cl, (ii) PAM, NEt_3, CH_3CN/borate buffer pH 9.5, (iii) ALN, HOBt/HBTU, NMM, DMF–H_2O, (iv) CF_3CO_2H. *Identification system for NMR assignments is displayed.*

downfield shifted (Δ = 7.2 ppm and 1.5 ppm, respectively) relatively to their position in free pamidronate (δ 17.5) and alendronate (δ 18.1). The magnitude of the chemical shifts is of the same order of those previously observed for other rhenium complexes of the same type (Δ = 3.4 ppm). These data confirm that the terminal bisphosphonic acid group is not involved in the coordination to the metal.[13] In addition, we also would like to underline that these shifts are far below those previously found for organometallic Re complexes that were directly stabilized by phosphonic acids (Δ = 16–30 ppm).[27]

The IR data indicated a facial arrangement of the carbonyl groups in **2** and **3**, with ν(CO) stretching bands in the range 2033–1912 cm^{-1}, as previously found for related complexes with the moiety "*fac*-$Re(CO)_3$".[13,25,26]

fac-[^{99m}Tc(CO)$_3$(pz-PAM)]$^-$ (2a) and *fac*-[^{99m}Tc(CO)$_3$(pz-ALN)]$^-$ (3a): radiosynthesis and characterization

The radioactive complexes [^{99m}Tc(CO)$_3$(pz-PAM)]$^-$ (**2a**) and [^{99m}Tc(CO)$_3$(pz-ALN)]$^-$ (**3a**) were prepared in high yield and radiochemical purity (> 95%) by reaction of *fac*-[^{99m}Tc(CO)$_3$(H$_2$O)$_3$]$^+$ with pz-PAM and pz-ALN, respectively (Scheme 2). The chemical identity of **2a** and **3a** has been ascertained by comparing their analytical RP-HPLC γ-traces with the RP-HPLC UV-vis traces of the rhenium analogs **2** and **3**. For the sake of example, we present in the ESI the RP-HPLC chromatograms obtained for **2** and **2a** (Fig. S1†).

The (lipo)hydrophilic nature of **2a** and **3a** was evaluated based on the octanol/0.1 M PBS pH 7.4 partition coefficients (log $P_{o/w}$). The average log $P_{o/w}$ values for three independent trials were −2.00 ± 0.02 (**2a**) and −1.94 ± 0.02 (**3a**), highlighting the strong hydrophilic character (log $P < -1$) of the complexes, which is certainly due to the presence of the pendant bisphosphonic acid groups. The overall charge of the radioactive complexes determined by electrophoresis (0.2 M phosphate buffered saline, pH 7.2) was found to be negative. Such a result can be explained by the deprotonation of the pendant bisphosphonates at pH 7.2 (Scheme 2)

To assess the potential of the resulting radioactive complexes as bone-seeking tracers, HA adsorption studies of **2a** and **3a** have been performed and their binding properties have been compared with those of ^{99m}Tc-MDP (Fig. 4).

Analysis of the adsorption curves (Fig. 4A) has shown that both complexes presented equivalent binding properties (maximum binding *ca.* 80% onto 20 mg of HA), which are comparable to those of ^{99m}Tc-MDP (maximum binding *ca.* 90% onto 20 mg of HA). In addition, we have also studied the binding kinetics of the three radiocompounds. The process is quite rapid for ^{99m}Tc-MDP, since the maximum adsorption (*ca.* 95%) was reached almost instantaneously (Fig. 4B). Complexes **2a** and **3a** presented a similar behaviour, but the

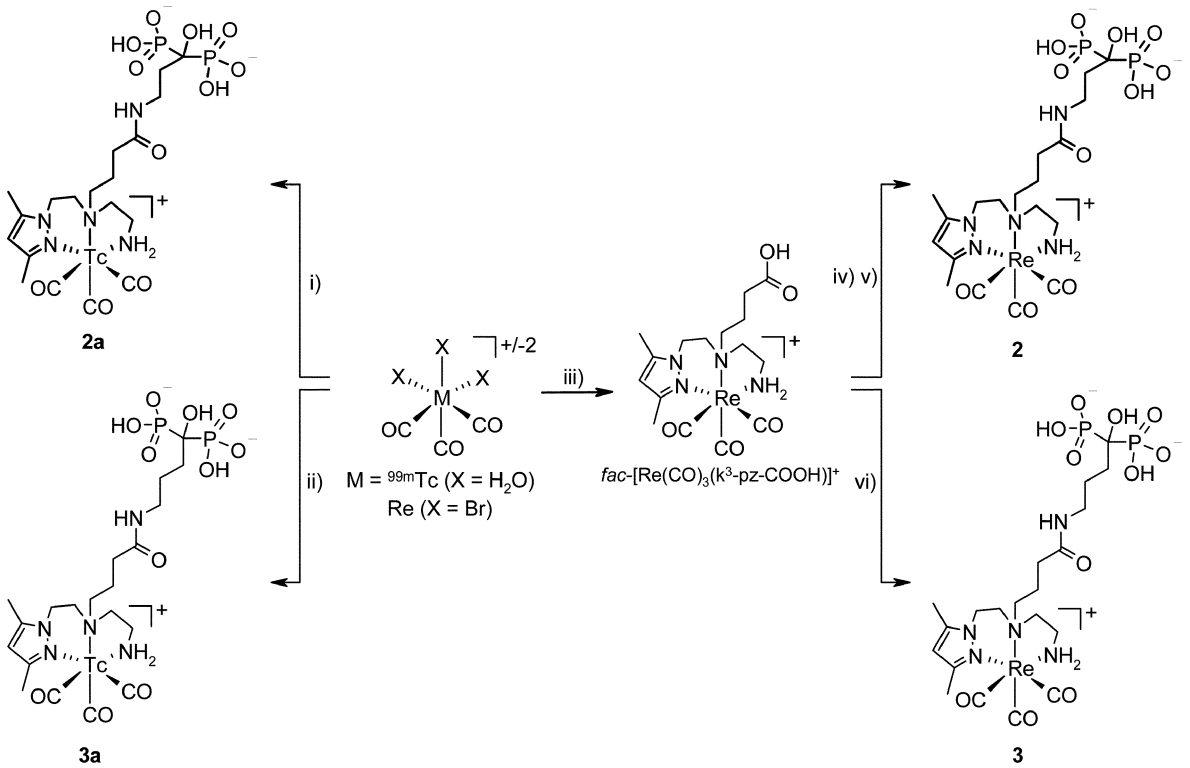

Scheme 2 Synthesis of **2**/**2a** and **3**/**3a**. (i) pz-PAM, H_2O, 100 °C, 30 min, (ii) pz-ALN, H_2O, 100 °C, 30 min, (iii) pz-COOH, H_2O, reflux, (iv) TFP/DCC, Acetonitrile, (v) PAM, NEt_3, Acetonitrile/borate buffer pH 9.4, (vi) ALN, HOBt/HBTU, NMM, DMF–H_2O.

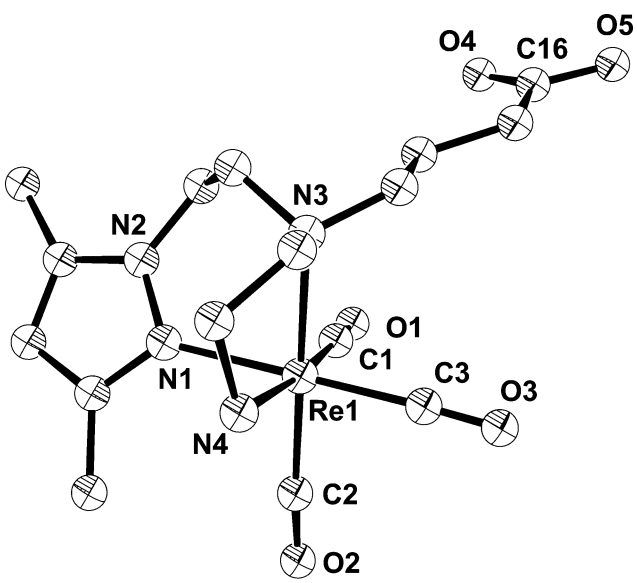

Fig. 3 ORTEP view of the cation *fac*-$[Re(CO)_3(k^3\text{-pz-COOH})]^+$ of molecule **1**. The H_2O solvate molecule, $CF_3CO_2^-$ counterion and H atoms are omitted for clarity. The vibrational ellipsoids are drawn at the 40% probability level. Selected bond distances and angles: Re1–C1 1.905(7) Å, Re1–C2 1.915(7) Å, Re1–C3 1.918(7) Å, Re1–N1 2.170(5) Å, Re1–N3 2.293(5) Å, Re1–N4 2.215(5) Å, C1–Re1–N1 90.0(2)°, C2–Re1–N1 95.1(2)°, C1–Re1–N3 98.8(2)°, C3–Re1–N3 92.8(2)°, C2–Re1–N4 96.2(2)°, C3–Re1–N4 94.4(2)°, C1–Re1–C2 86.3(3)°, C1–Re1–C3 91.3(3)°, N1–Re1–N3 86.57(18)°, N1–Re1–N4 84.22(19)°.

maximum adsorption onto HA was only reached after 4 h (*ca.* 80%).

Biodistribution and imaging studies

The bone-seeking properties and biological profile of **2a** and **3a** were assessed in normal Balb-c mice at 1 h and 4 h after intravenous injection (Fig. 5A). For comparison, we have also evaluated, in the same animal model, the tissue distribution profile of ^{99m}Tc-MDP, the most widely used bone-imaging radiopharmaceutical. Total radioactivity excretion at both time points was also determined for all the ^{99m}Tc-complexes (Fig. 5B).

These studies showed that **2a** and **3a** were rapidly taken by bone with a long residence time. Both complexes were quite efficiently cleared from the blood stream and soft tissues with no significant radioactivity accumulation in any major organ, except those involved in the excretory routes (kidneys, liver and intestines). Nevertheless, the liver uptake was slightly lower (**2a**: 2.3 ± 0.1% I.D./g and **3a**: 1.8 ± 0.1% I.D./g, at 1 h post injection) than that found for ^{99m}Tc-MDP (3.7 ± 0.6% I.D./g, at 1 h post injection). The bone-uptake of **2a** (18.3 ± 0.6% I.D./g) and **3a** (17.3 ± 6.1% I.D./g) is comparable to the values found for ^{99m}Tc-MDP (17.1 ± 2.4% I.D./g) at 1 h post injection. Unlike ^{99m}Tc-MDP, there was a slight decrease in the bone uptake at 4 h post injection. However, the percentage of the total excretion from the whole animal body (Fig. 5B) of **2a** and **3a** (**2a**: 66.8 ± 7.6% I.D., 77.2± 0.5% I.D. and **3a**: 65.6 ± 1.2% I.D, 74.1 ± 0.9% I.D., at 1 h and 4 h post injection, respectively) was significantly higher than that of ^{99m}Tc-MDP (49.0 ± 6.1% I.D., 56.8 ± 0.9% I.D., at 1 h and 4 h post injection, respectively). Accordingly, compared to ^{99m}Tc-MDP, the bone-to-blood and bone-to-muscle ratios of **2a** and **3a** increased overtime (Fig. 6).

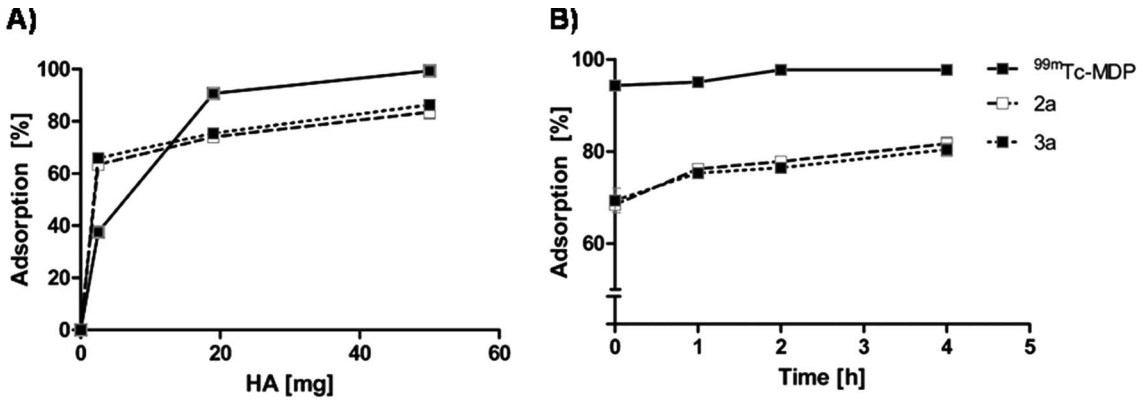

Fig. 4 Adsorption curves of ^{99m}Tc-MDP, **2a** and **3a** onto HA as a function of HA amount (**A** 1h, 37 °C) and incubation time (**B** 20 mg HA, 37 °C).

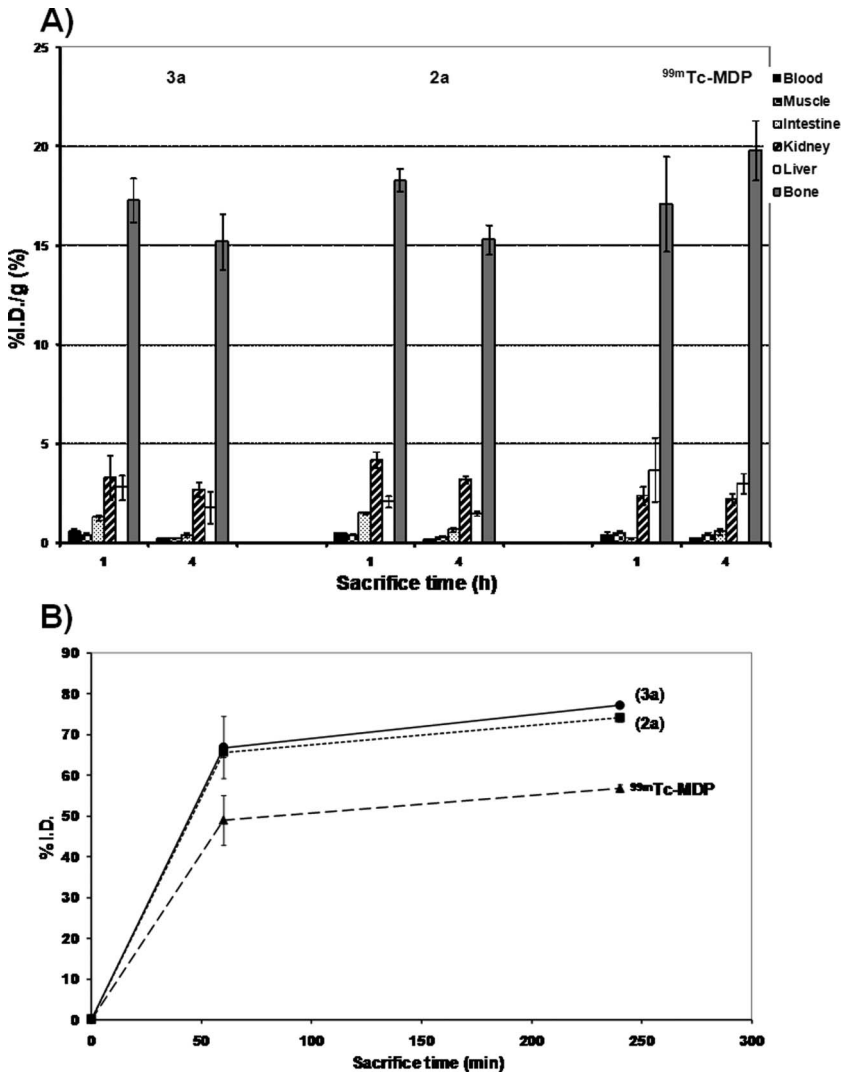

Fig. 5 Radioactivity biodistribution (**A**) and total radioactivity excretion profile (**B**) of **2a**, **3a** and ^{99m}Tc-MDP in adult Balb-c female mice ($n = 4$).

The RP-HPLC analysis of urine and blood samples collected at sacrifice (1 h post injection) indicated that **2a** and **3a** are stable *in vivo*.

Whole body images of Sprague Dawley rats acquired at 2 h after injection of **2a**, **3a** and ^{99m}Tc-MDP are presented in Fig. 7.

As expected from the biodistribution results in Balb-b mice, both tracers allowed a clear visualization of the skeleton, demonstrating a high bone uptake especially in the joints, owing to the higher remodelling activity. All other organs presented a very low uptake. The scintigraphic images obtained with **2a** and **3a**

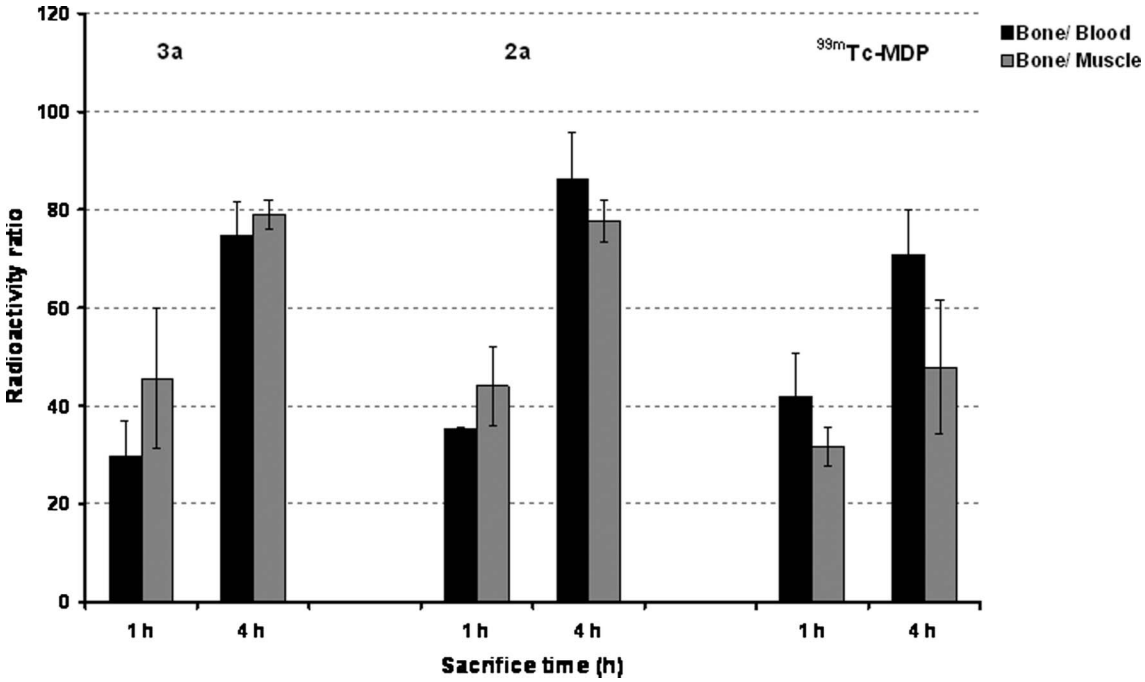

Fig. 6 Bone-to-blood and bone-to-muscle ratios of **2a**, **3a** and ^{99m}Tc-MDP ($n = 4$) in adult Balb-c female mice.

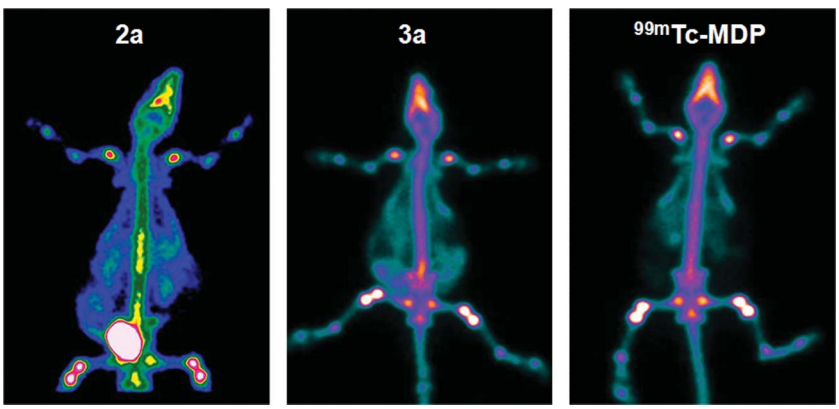

Fig. 7 Planar whole-body gamma camera images of rats injected with **2a**, **3a** and ^{99m}Tc-MDP, 2 h after administration.

displayed good quality and are quite similar to that of ^{99m}Tc-MDP, confirming the potential usefulness of **2a** and **3a** as bone-seeking agents.

Conclusions

The labelling of the well-known bisphosphonates pamidronate and alendronate with "$^{99m}Tc(CO)_3$", following a bifunctional approach, resulted in the preparation of the well-defined radioactive complexes *fac*-[$^{99m}Tc(CO)_3$(pz-PAM)]$^-$ (**2a**) and *fac*-[$^{99m}Tc(CO)_3$(pz-ALN)]$^-$ (**3a**) in high yield and radiochemical purity. Comparative analysis of the biodistribution profiles of **2a** and **3a** with that of ^{99m}Tc-MDP, demonstrated that both complexes have a similar high bone uptake and clearance from most tissues and an increased total excretion. Consequently, the bone-to-blood and the bone-to-muscle ratios are significantly higher than that of ^{99m}Tc-MDP, especially in the case of **2a**. The imaging studies using Sprague Dawley rats confirmed that **2a** and **3a** allow a clear visualization of the skeleton with low uptake in any other organ. Taken together, the high bone uptake, favourable bone-to-blood and bone-to-muscle ratios and high *in vivo* stability of **2a** and **3a** make them highly promising candidates for bone-imaging. Whether these new radioactive complexes can have an impact in nuclear medicine has still to be clinically evaluated.

Experimental

General procedures and materials

All chemicals and solvents were of reagent grade and were used without purification, unless stated otherwise. The Boc-protected bifunctional chelator 4-((2-(*tert*-butoxycarbonylamino)ethyl)(2-(3,5-dimethyl-1*H*-pyrazol-1-yl)ethyl)amino)butanoic acid (pz(Boc)–COOH) (Boc = *tert*-butoxycarbonyl) and $(NEt_4)_2[ReBr_3(CO)_3]$ were prepared according to published methods.[13,26,28] (3-Amino-1-hydroxypropylidene)bisphosphonic

acid monohydrate (Pamidronate, PAM) and (4-Amino-1-hydroxybutylidene)bisphosphonic acid trisodium salt tetrahydrate (Alendronate, ALN) were synthesized according to the procedure of Kieczykowski *et al.*[29] The purification of some bisphosphonate compounds was achieved by using Sep Pak C18 cartridges (Waters Co., 12 cc/2 g or 0.85 cc/360 mg) preconditioned according to the manufacturer's protocol and eluted using a H_2O–MeOH gradient. Elution of the products started with water, followed by mixtures of MeOH–H_2O (20–100%). The presence of bisphosphonates in the elution fractions was monitored by TLC, using the Dittmer's reagent as the revelator agent.[30]

^1H, ^{13}C and ^{31}P NMR spectra were recorded at room temperature using a Varian Unity 300 MHz spectrometer. ^1H and ^{13}C chemical shifts were referenced with the residual solvent resonances relative to $SiMe_4$ and the ^{31}P chemical shifts with external 85% H_3PO_4 solution. NMR spectra were obtained in D_2O. The spectra were assigned with the help of 2D experiments (^1H–^1H correlation spectroscopy, COSY and ^1H–^{13}C heteronuclear single quantum coherence, HSQC). IR spectra were recorded as KBr pellets on a Bruker Tensor 27 spectrometer. C, H and N analyses were performed using an EA 110 CE Instruments automatic analyser. Compounds were characterized by electrospray ionization mass spectrometry (ESI-MS) using a QITMS instrument. Na[$^{99m}TcO_4$] was eluted from a $^{99}Mo/^{99m}Tc$ generator, using 0.9% saline. The radioactive precursor *fac*-[$^{99m}Tc(CO)_3(H_2O)_3]^+$ was prepared using an IsoLink® kit (Covidean/Malinckrodt). ^{99m}Tc-MDP (better than 98% yield by instant thin-layer chromatography) was prepared by reconstitution of a conventional MDP labelling kit (Nordion and GE) with Na[$^{99m}TcO_4$].

Reversed-phase high performance liquid chromatography (RP-HPLC) analyses of the M(I)-complexes (M = Re, ^{99m}Tc) were performed with a Perkin Elmer LC pump 200 coupled to a LC 290 tunable UV–vis detector and to a Berthold LB-507A radiometric detector. A Macherey-Nagel C18 reversed-phase column (Nucleosil 10 μm, 250 × 4 mm) was used. HPLC solvents consisted of 0.5% CF_3COOH in H_2O (solvent A) and 0.5% CF_3COOH solution in acetonitrile (solvent B), gradient: t = 0–3 min, 0% eluent B; 3–3.1 min, 0–25% eluent B; 3.1–9 min, 25% eluent B; 9–9.1 min, 25–34% eluent B; 9.1–20 min, 34–100% eluent B; 20–24 min, 100% eluent B; 24–26 min, 100–0% eluent B; 26–30 min, 0% eluent B. Purification of the rhenium precursor *fac*-[$Re(CO)_3(k^3$-pz-COOH)]$^+$ was achieved on a semi-preparative Macherey–Nagel C18 reversed-phase column (Nucleosil 100–7, 250 × 8 mm) with a flow rate of 2.0 mL min^{-1}, using the above described gradient. UV detection: 220 nm. Eluents: A = aqueous 0.1% CF_3COOH and B = MeOH. Alternatively, the rhenium precursor *fac*-[$Re(CO)_3(k^3$-pz-COOH)]$^+$ could also be purified with Sep-Pak C18 cartridges according to the above described method.

Dittmer reagent.[30]

Solution I. A mixture of molybdic oxide (4 g) in conc. H_2S0_4 (100 mL) was boiled gently with magnetic stirring until a clear solution was obtained.

Solution II. To solution I (50 mL) was added powdered molybdenum (0.180 g), which was dissolved by heating.

Stock solution. After cooling, solution I (50 mL) was mixed with an equal volume of solution II. This solution remained stable at least for one year in a closed vial.

For detection of bisphosphonate compounds in silica gel plates, stock solution (2.5 mL) was diluted with water (5 mL) and ethanol (7.5 mL). The plates were sprayed uniformly with Dittmer reagent until lightly damp in a fume hood. After heating on a hot plate (100 °C), bisphosphonates gave sharp blue spots which increased intensity after 10 to 15 min standing at room temperature. An initial dark blue coloration of the background disappeared to give a uniform white background with sharp blue spots.

Synthesis of pz-PAM

To a solution of pz(Boc)-COOH (0.200 g, 0.54 mmol) and *N*-hydroxysuccinimide (NHS) (0.075 g, 0.65 mmol) in dry dichloromethane (4 mL) was added dropwise *N*,*N*′-dicyclohexylcarbodiimide (DCC; 0.134 g, 0.65 mmol) at room temperature and the reaction mixture was stirred for 5 h. The DCC-urea precipitate was removed by filtration and the solvent of the filtrate evaporated. The residue obtained was dissolved in acetonitrile (3.5 mL) and used in the next reaction without further purification. The acetonitrile solution was added dropwise to a suspension of PAM (0.209 g, 0.82 mmol) in a solution of triethylamine (3.5 mL) and water (150 μL). The reaction mixture was stirred at room temperature and, after 24 h, the unreacted PAM was discarded by centrifugation. The supernatant was evaporated and the residue was chromatographed on an appropriate silica gel column using CH_2Cl_2, 10–100% methanol/$CHCl_3$ (gradient) and 25–100% concentrated aqueous ammonia/methanol (gradient) as eluents to remove the unreacted starting reagents and remaining DCC-urea. Pz(Boc)-PAM was the last compound to be eluted and, after evaporation of the elution solvent, was obtained as a colourless oil. Yield: 0.070 g, 22%. ^1H NMR (D_2O, δ (ppm)): 5.82 (s, H(4)pz, 1H), 4.07 (s br, CH_2, 2H), 3.32 (t, CH_2, 2H), 3.12 (m, CH_2, 2H), 2.79–2.72 (overlapped m, CH_2, 4H), 2.24 (m, CH_2, 2H), 2,11 (overlapped m, CH_2 and CH_3, 5H), 2.02 (overlapped m, CH_2 and CH_3, 5H), 1.69 (m, CH_2, 2H), 1.25 (s, CH_3, 9H). ^{31}P NMR (D_2O, δ (ppm)): 18.34. A solution of Pz(Boc)-PAM (0.070 g, 0,12 mmol) in CF_3COOH (2 mL) was stirred for 1 h at room temperature. After evaporation of the solvent, the residue was dissolved in water (1 mL) and purified on a strongly acidic cation-exchange resin (Dowex 50 × 4, elution with water followed by 10% aqueous pyridine). After evaporation of the solvents, the residue was dissolved in water and applied to a weakly acidic cation-exchange resin (Amberlite CG50, elution with water) in order to remove the remaining pyridine. The product-containing fractions were collected and, after evaporation of the solvent, afforded pz-PAM as a colourless oil. Yield: 0.0176 g, 30%. ^1H NMR (D_2O, δ (ppm)): 5.88 (s, H(4)pz, 1H), 4.21 (t, J_{HH} = 5.8 Hz, CH_2^a, 2H), 3.34 (overlapped m, CH_2^b and CH_2^h, 4H), 3.19 (overlapped m, CH_2^c and CH_2^d, 4H), 2.92 (t, J_{HH} = 6.6, CH_2^g, 2H), 2.19 (t, J_{HH} = 6.9, CH_2^e, 2H), 2.14 (s, CH_3pz, 3H), 2.04 (s, CH_3 pz, 3H), 1.99 (m, CH_2^i, 2H), 1.76 (m, CH_2^f, 2H). ^{13}C NMR (D_2O, δ (ppm)): 176.5 (C═O), 151.6 (C(3/5)pz), 144.1 (C(3/5)pz), 108.2 (C(4)pz), 74.85 (C–OH), 55.30 (CH_2^g), 54.34 (CH_2^b) 52.07 (CH_2^c), 45.13 (CH_2^a), 37.48 (CH_2^h), 36.79 (CH_2^d), 34.74 (CH_2^e + CH_2^i), 22.0 (CH_2^f), 14.2 (CH_3pz), 12.0 (CH_3pz). ^{31}P NMR (D_2O, δ (ppm)): 18.2. ESI-MS [+]: calcd for $C_{16}H_{34}N_5O_8P_2$ $[M + H]^+$ 486.2, found 486.0. Calcd for $C_{16}H_{33}N_5NaO_8P_2$ $[M + Na]^+$ 508.2, observed 507.9. Calcd for $C_{16}H_{33}N_5KO_8P_2$ $[M + K]^+$ 524.2, observed 523.9. ESI-MS [–]: Calcd for $C_{16}H_{32}N_5O_8P_2$ $[M - H]^-$ 484.2, observed 484.1. Anal.

calcd for $C_{16}H_{32}N_5NaO_8P_2{\cdot}2H_2O$: C 35.36%, H 6.68%, N 12.89%. Found: C 35.60%, H 6.54%, N 13.20%.

Pz-ALN

A solution of ALN (0.092 g, 0.283 mmol) and 4-methylmorpholine (NMM; 190 µl, 1.74 mmol) in H_2O (5 mL) was added dropwise to a solution of pz(Boc)-COOH (0.064 g, 0.174 mmol), 1-hydroxybenzotriazole hydrate (HOBt; 0.070 g, 0.521 mmol) and O-benzotriazol-*N*,*N*,*N*′,*N*′-tetramethyluronium-hexafluoro phosphate (HBTU; 0.198 g, 0.521 mmol) in DMF (5 mL). The final pH was adjusted to 8 by adding extra NMM (95 µl, 0.87 mmol). The reaction mixture was stirred at room temperature for 5 d and the white precipitate corresponding to unreacted ALN was separated by centrifugation. The supernatant was vacuum dried and the residue was dissolved in water (2 mL), precipitating excess HOBt/HBTU as thin crystals. The precipitate was separated by filtration and the filtrate was loaded onto a conditioned Sep-Pak C18 cartridge (Waters, 12 cc, 2 g) and washed with water. The conjugated compound pz(Boc)-ALN and some free starting material were eluted with 50% methanol. After removing the solvent, the obtained residue was further purified on an appropriate silica gel column eluted with CH_2Cl_2, 10–100% methanol–$CHCl_3$ (gradient) and 25–100% concentrated aqueous ammonia/methanol (gradient), affording pz(Boc)-ALN as a colourless oil. Yield: 0.012 g, 12%. ^{1}H NMR (D_2O, δ (ppm)): 5.84 (s, H(4)pz, 1H), 4.07 (t, CH_2^a, 2H), 3.09 (overlapped m CH_2, 6H), 2.78 (t, CH_2, 2H), 2.68 (t, CH_2^g, 2H), 2.14 (overlapped m, CH_2^e and CH_3, 5H), 2.04 (s, CH_3pz, 3H), 1.81–1.68 (overlapped m, CH_2, 6H), 1.28 (s, CH_3(BOC), 9H. ^{31}P NMR (D_2O, δ (ppm)): 18.6. ^{13}C NMR (D_2O, δ (ppm)): 177.4 (C═O), 160.08 (C═O, BOC), 151.2 (C(3/5)pz), 143.7 (C(3/5)pz), 107.4 (C(4)pz), 83.2 (C–OH), 54.6–54.4 (overlapped (CH_2^c, CH_2^d, CH_2^g), 46.1 (CH_2^a), 42.2 (CH_2), 38.7(CH_2), 35.0 (CH_2^e), 33.3 (CH_2), 29.6 (CH_3, BOC), 25.5 (CH_2), 23.3(CH_2), 14.2 (CH_3pz), 12.1 (CH_3pz).

A solution of pz(Boc)-ALN (0.012 g, 0.020 mmol) in CF_3COOH (2 mL) was stirred at room temperature for 1 h. Thereafter, the solvent was evaporated and the resulting residue was dissolved in water (5 mL) and neutralized with NaOH 0.1 M. The volume of the obtained solution was reduced to 1 mL and the concentrate was purified on a conditioned Sep Pak C18 cartridge (Waters, 12 cc, 2 g). The first 2 mL, containing mainly CF_3COONa salts were discarded, and pz-ALN was eluted with H_2O (4 mL). Yield: 0.004 g, 40%. ^{1}H NMR (D_2O, δ (ppm)): 5.79 (s, H(4)pz, 1H), 3.92 (t, CH_2^a, 2H), 3.04 (m, CH_2, 2H), 2.72 (overlapped m, CH_2,4H), 2.51 (m, CH_2, 2H), 2.36 (m, CH_2, 2H), 2.11 (s, CH_3pz, 3H), 2.01 (overlapped m, CH_2^e and CH_3, 5H), 1.76–1.57 (overlapped m, CH_2, 6H). ^{31}P NMR (D_2O, δ (ppm): 18.3. ESI-MS [–] *m*/*z*: calcd for $C_{17}H_{35}N_5O_8P_2$ $[M]^-$ 499.2, observed 499.3. Calcd for $C_{17}H_{33}N_5O_8P_2$ $[M-2H]^{2-}$ 448.6, observed 449.1. Calcd for $C_{17}H_{34}N_5NaO_8P_2$ $[M-H+Na]^-$: 521.2, observed 521.3. Anal. calcd for $C_{17}H_{34}N_5NaO_8P_2{\cdot}H_2O$: C 37.85%, H 6.73%, N 12.98%. Found: C 37.02%, H 6.92%, N 12.73%.

Synthesis of *fac*-[Re(CO)$_3$(k^3-pz-COOH)]$^+$

The complex has been synthesized as previously described, starting with $(NEt_4)_2[ReBr_3(CO)_3]$ in refluxing water.[13,26] When the crude residue was purified by Sep-Pak C18 cartridges (Waters, 0.85 cc/360 mg) the species *fac*-[Re(CO)$_3$(k^3-pz-COOH)]Br was obtained as a viscous colourless oil. Alternatively, the species *fac*-[Re(CO)$_3$(k^3-pz-COOH)]$^+{\cdot}CF_3COO^-$ was obtained when the crude residue was purified by preparative RP-HPLC. Suitable crystals of *fac*-[Re(CO)$_3$(k^3-pz-COOH)]$^+{\cdot}$ $CF_3COO^-{\cdot}H_2O$ for single-crystal X-ray diffraction analysis were grown by slow diffusion of $CHCl_3$ into a methanolic solution of the purified compound (see X-ray crystallographic analysis section).

Synthesis of *fac*-[Re(CO)$_3$(pz-PAM)]$^-$ (2)

To a solution of *fac*-[Re(CO)$_3$(k^3-pz-COOH)]Br (0.039 g, 0.063 mmol) and tetrafluorophenol (TFP; 0.023 g, 0.138 mmol) in dry acetonitrile (4 mL) at 0–5 °C was added DCC (0.028 g, 0.138 mmol). The mixture was stirred for 14 h. The DCC–urea precipitate was removed by centrifugation and the resulting solution evaporated. The residue was then suspended in an adequate volume of ethyl acetate, the remaining DCC urea was removed by filtration and the filtrate was evaporated in vacuo. The crude residue was dissolved in acetonitrile (2.5 mL), filtered to discard the remaining DCC–urea and added to a solution of PAM (0.017 g, 0.067 mmol) in 2.5 mL of 0.1 M borate buffer (pH 9.4) and triethylamine (60 µL). The final pH value was about 9 and the reaction mixture was stirred for five d at room temperature. The mixture was concentrated to dryness, the resulting residue was extracted with water and, after removing the supernatant's solvent under vacuum, the residue was washed with acetonitrile to remove excess NEt_3. Complex **2** was obtained in a pure form after purification with Sep-Pak C18 cartridges (2 × Waters, 0.85 cc/360 mg). $[Re(CO)_3(pz\text{-}PAM)]^-$ (**2**) was eluted with 25–75% methanol/H_2O (gradient) after washing the cartridge with H_2O (10 mL). Yield 0.014 g, 24%.^{1}H NMR (D_2O, δ (ppm)): 6.07 (s, H(4)pz, 1H), 5.11 (m, NH, 1H), 4.36 (dd, $^2J_{HH}$ = 15.8 Hz, $^3J_{HH}$ = 3.2 Hz, CH^a, 1H), 4.13 (dd, $^2J_{HH}$ = 15.8 Hz, $^3J_{HH}$ = 10.6 Hz, $CH^{a\prime}$, 1H), 3.64 (m, NH, 1H), 3.54 (dd, $^2J_{HH}$ = 12.4 Hz, $^3J_{HH}$ = 3.5 Hz, CH^g, 1H), 3.42–3.37 (m, $CH_2^h/^{h\prime}$+ $CH^{g\prime}$ + CH^b, 4H), 3.11 (m, CH^d, 1H), 2.76 (m, $CH_2^{c/c\prime}$, 2H), 2.60 (dd, $^2J_{HH}$ = 14.4 Hz, $^3J_{HH}$ = 10.8 Hz, $CH^{b\prime}$, 1H), 2.43 (m, $CH^{d\prime}$, 1H), 2.30 (s, CH_3pz, 3H), 2.19 (m, CH_3pz + $CH_2^{e/e\prime}$, 5H), 2.13–1.89 (m, $CH_2^{f/f\prime}$ + $CH_2^{i/i\prime}$, 4H). ^{13}C NMR (D_2O, d): 194.6, 194.2, 193.1 (C≡≡O), 174.9 (C═O), 153.7 (C(3/5)pz), 144.3 (C(3/5)pz), 107.8 (C(4)pz), 73.2 (t, J_{CP} = 129.4 Hz, C^j), 66.0 (C^g), 61.3 (C^c), 52.8 (C^b), 47.2 (C^a), 42.2 (C^d), 36.1 (t, J_{CP} = 7.9 Hz, C^h), 33.1 (C^e + C^i), 20.7 (C^f), 15.4 (CH_3pz), 10.9 (CH_3pz). ^{31}P NMR (D_2O, δ (ppm)): 24.67. IR (KBr, ν/cm^{-1}): 2033, 1927, 1913 (C≡≡O), 1686, 1442, 1210, 1141, 845, 803, 726. ESI-MS [–] *m*/*z*: calcd for $ReO_{11}N_5C_{19}H_{30}P_2$ $[M-3H]^{2-}$ 376.5, observed 376.5. Calcd for $ReO_{11}N_5C_{19}H_{31}P_2$ $[M-2H]^-$ 754.1, observed 753.9. Calcd for $ReO_{11}N_5C_{19}H_{30}P_2Na$ $[M\text{-}3H+Na]^-$ 776.1, observed 775.9. Calcd for $ReO_{11}N_5C_{19}H_{30}P_2K$ $[M\text{-}3H+K]^-$ 792.1, observed 791.9. Anal. calcd for $C_{19}H_{31}N_5Na_2O_{11}P_2ReBr{\cdot}CH_3OH$: C 26.35%, H 3.87%, N 7.68%. Found: C 26.45%, H 3.74%, N 7.66%.

Synthesis of *fac*-[Re(CO)$_3$(pz-ALN)]$^-$ (3)

A solution of ALN (0.017 g, 0.052 mmol) and NMM (36 µl, 0.325 mmol) in H_2O (2 mL) was added dropwise to a solution of *fac*-[Re(CO)$_3$(k^3-pz-COOH)]Br (0.025 g, 0.040 mmol), 1-hydroxybenzotriazole hydrate (HOBt; 0.013 g, 0.097 mmol)

and O-benzotriazol-*N*,*N*,*N*′,*N*′-tetramethyluronium-hexafluoro phosphate (HBTU; 0.037 g, 0.097 mmol) in DMF (2 mL). The final pH was adjusted to 8 by adding NMM (18 μL, 0.163 mmol). The reaction mixture was stirred at room temperature and, after five d, the solvent was removed under vacuum and the residue was extracted with water (*ca.* 5 mL). This volume was reduced to 2 mL and the concentrate was loaded on a conditioned Sep Pak cartridge (waters, 12 cc, 2 g). *fac*-[$Re(CO)_3$(pz-ALN)]$^-$ was eluted with a mixture of 50% methanol/H_2O after washing the cartridge with small amounts of H_2O, 20% methanol/H_2O and 30% methanol/H_2O. Yield: 0.015 g; 40%. ^{1}H NMR (D_2O, δ (ppm)): 6.02 (s, H(4)pz, 1H), 5.06 (m, NH, 1H), 4.31 (dd, $^2J_{HH}$ = 25.7 Hz, $^3J_{HH}$ = 3.0 Hz CH^a, 1H), 4.08 (dd, $^2J_{HH}$ = 15.4 Hz, $^3J_{HH}$ = 11.0 Hz, $CH^{a'}$, 1H), 3.64 (m, NH, 1H), 3.50 (m, CH^g, 1H), 3.29–3.26 (m, CH_2^b + $CH^{g'}$, 2H), 3.08–3.06 (m, $CH^{h\,h-1'}$+ CH^d, 1H), 2.71 (m, $CH_2^{c/c'}$, 2H), 2.56 (m, $CH^{b'}$, 1H), 2.38 (m, $CH^{d'}$, 1H), 2.26 (s, CH_3pz, 3H), 2.21–2.15 (m, $CH_2^{e/e'}$ + CH_3pz, 5H), 2.11–2.03 (m, $CH_2^{f/f'}$, 2H), 1.89–1.750 (m, CH_2^j, 2H), 1.755–1.655 (m, CH_2^i, 2H). ^{13}C NMR (D_2O, d): 194.55, 194.21, 193.06 (C≡O), 175.37 (C═O), 153.68 [C(3/5)pz], 144.3 [C(3/5)pz], 107.7 [C(4)pz], 71.8 (C^k), 65.9 (C^g), 61.3 (C^c), 52.8 (C^b), 47.1 (C^a), 42.2 (C^d), 40.0 (C^h), 32.8 (C^e), 31.1 (C^j), 23.3 (m, C^i), 20.7 (C^f), 15.3 (CH_3pz), 10.9 (CH_3pz). ^{31}P NMR (D_2O, δ (ppm)): 19.6. IR (KBr, ν/cm^{-1}): 2026, 1930 (sh), 1912 (C≡O), 1650 (C═ONH), 1172, 1064, 526. ESI-MS [–] *m*/*z*: calcd for $C_{20}H_{32}N_5O_{11}P_2Re$ $[M - 3H]^{2-}$ 383.5, observed 383.4. Calcd for $C_{20}H_{33}N_5O_{11}P_2Re$ $[M - 2H]^-$ 768.1, observed 768.0. ESI-MS [+] *m*/*z*: calcd for $C_{20}H_{35}N_5O_{11}P_2Re$ $[M]^+$ 770.1, observed 770.1. Calcd for $C_{20}H_{34}N_5O_{11}P_2ReNa$ $[M - H + Na]^+$ 792.1, observed 792.1. Calcd for $C_{20}H_{33}N_5O_{11}P_2ReNa_2$ $[M - 2H + 2Na]^+$ 814.1, observed 814.1. Calcd for $C_{20}H_{33}N_5O_{11}P_2ReKNa$ $[M - 2H + Na + K]^+$ 830.1, observed 830.0. Anal. calcd for $C_{20}H_{33}N_5Na_2O_{11}P_2ReBr{\cdot}CH_3OH$: C 27.25%, H 4.03%, N 7.57%. Found: C 27.76%, H 4.19%, N 7.31%.

X-Ray crystallographic analysis

Single-crystal X-ray diffraction analysis has been performed on a Bruker AXS APEX CCD area detector diffractometer, using graphite monochromated Mo Ka radiation (0.71073 Å). Empirical absorption correction was carried out using SADABS.[31] Data collection and data reduction were done with the SMART and SAINT programs.[32] The structure was solved by direct methods with SIR97 and refined by full-matrix least-squares analysis with SHELXL-97 using the WINGX suite of programmes.[33–35] All non-hydrogen atoms were refined anisotropically. The remaining hydrogen atoms were placed in calculated positions. Molecular graphics were prepared using ORTEP3.[36] A summary of the crystal data, structure solution and refinement parameters is given in ESI (Table S1†) and selected bond lengths and angles appear in Fig. 3. Complex *fac*-[$Re(CO)_3(k^3$-pz-COOH)]$^+{\cdot}CF_3COO^-{\cdot}H_2O$ crystallized with three independent molecules per asymmetric unit, which can be considered to be chemically equivalent.

Synthesis of *fac*-[^{99m}Tc(CO)$_3$(pz-PAM)]$^-$ (2a) and *fac*-[^{99m}Tc(CO)$_3$(pz-ALN)]$^-$ (3a)

In a nitrogen-purged glass vial, 100 μL of a 10^{-3} M solution of pz-PAM or pz-ALN in distilled water were added to 900 μL of a solution of *fac*-[$^{99m}Tc(CO)_3(H_2O)_3]^+$ (185 MBq) in saline pH 7.4. The reaction mixtures were heated at 100 °C for 30 min, cooled on an ice bath and then analyzed by RP-HPLC: t_R = 12.0 min (**2a**), 11.9 min (**2**); t_R = 14.2 min (**3a**), 13.8 min (**3**).

Complex charge and partition coefficient

The overall charge of the complexes in 0.2 M phosphate buffered saline pH 7.2 was determined by electrophoresis as previously described.[37]

The lipophilicity of the radioconjugate was evaluated by the "shakeflask" method.[38] Briefly, the radioconjugates were added to a mixture of octanol (1 mL) and 0.1 M PBS pH = 7.4 (1 mL), previously saturated in each other by stirring the mixture. This mixture was vortexed and centrifuged (3000 rpm, 10 min, room temperature) to allow phase separation. Aliquots of both octanol and PBS were counted in a gamma counter. The partition coefficient ($P_{o/w}$) was calculated by dividing the counts in the octanol phase by those in the buffer, and the results expressed as Log $P_{o/w}$. Log $P_{o/w} = -2.00 \pm 0.02$ (**2a**). Log $P_{o/w} = -1{,}94 \pm 0.02$ (**3a**)

Hydroxyapatite (HA) binding

Adsorption of **2a**, **3a** and ^{99m}Tc-MDP onto HA was accomplished following an adaptation of previously described methods.[39] Briefly, 50 μL of each complex (~11.1 MBq/500 μL) were incubated for 1 h at 37 °C in a water bath with 2.5, 10 and 50 mg of solid HA and 500 μL of phosphate buffered saline (PBS) solution (pH 7.2). The liquid and solid phases were separated by centrifugation (7500 rpm/3 min) and the solid phase washed twice with 500 μL of PBS solution (pH 7.2). The activity in the liquid and solid phases was determined using an ionization chamber.

Alternatively, the adsorption of the ^{99m}Tc complexes onto HA along time incubation at 37 °C was also determined. For that, 50 μL of each complex (~11.1 MBq/500 μL) were incubated for 0, 1, 2 and 4 h at 37 °C in a water bath with 20 mg of solid HA and 500 μL of phosphate buffered saline (PBS) solution (pH 7.2). The liquid and solid phases were treated as described above.

Biodistribution studies

The *ex-vivo* biodistribution of the complexes was evaluated in groups of four adult Balb-c female mice (Charles River) weighing approximately 15 g each. The animals were injected intravenously with 100 μL (22–32 MBq) of each preparation *via* the tail vein and were maintained on normal diet ad libitum. All animal studies were conducted in accordance with the highest standards of care, as outlined in European law. Mice were killed by cervical dislocation at 1 and 4 h after injection. The injected radioactive dose and the radioactivity remaining in the animal at sacrifice were measured with a dose calibrator (Aloka, Curiemeter IGC-3, Tokyo, Japan). The difference between the radioactivity in the injected and the sacrificed animal was assumed to be due to total excretion from whole animal body. Blood samples were taken by cardiac puncture when the animals were killed. Tissue samples of the main organs were removed, weighed and counted using a γ counter (Berthold). Biodistribution results were expressed as the percentage of the injected dose (ID) per gram of tissue.

Statistical analysis of the biodistribution data (t-test) was done with GraphPad Prism and the level of significance was set as 0.05.

In vivo stability

The stability of the complexes was assessed in urine and murine serum by RP-HPLC analysis under identical conditions to those used for analyzing the original radiolabelled complexes. The samples were taken 1 h post injection. The urine collected at the sacrifice time was filtered through a Millex GV filter (0.22 μm) before RP-HPLC analysis. Blood collected from the mice was centrifuged at 3000 rpm for 15 min at 4 °C and the serum was separated. The serum was treated with ethanol in a 2 : 1 (v/v) ratio to precipitate the proteins. After centrifugation at 3000 rpm for 15 min at 4 °C, the supernatant was collected, filtered through a Millex GV filter (0.22 μm) and analysed by RP-HPLC.

Imaging

A set of Sprague Dawley rats were intravenously injected with 37 MBq of each ^{99m}Tc(I)-complex or with ^{99m}Tc-MDP for comparison. Whole-body images of the rats were obtained with a GE gamma camera connected to a Starcam 4000i computer. All the images were acquired in a 128 × 128 matrix at 2 h after administration of the ^{99m}Tc(I)-complexes and ^{99m}Tc-MDP.

Acknowledgements

This work has been supported by the Fundação para a Ciência e Tecnologia (FCT) through the project PTDC/QUI-QUI/115712/2009. Partial support through COST ACTIONS D38 and D39 is acknowledged. We thank Covidean for providing the IsoLink® links. E. Palma and B. L. Oliveira thank FCT for the PhD grants SFRH/BD/29527/2006 and SFRH/BD/38753/2007, respectively. Dr J. Marçalo is acknowledged for performing the ESI-MS analyses. The QITMS instrument was acquired with the support of the Programa Nacional de Reequipamento Científico (REDE/1503/REM/2005 - ITN) of FCT and is part of Rede Nacional de Espectrometria de Massa. Dr G. Cantinho and Mr. V. Marques are acknowledged for the gamma camera imaging studies with Sprague-Dawley rats.

Notes and references

1 R. G. Russell, R. C. Muhlbauer, S. Bisaz, D. A. Williams and H. Fleisch, *Calcif. Tissue Res.*, 1970, **6**, 183–196.
2 M. T. Drake, B. L. Clarke and S. Khosla, *Mayo Clin. Proc.*, 2008, **83**, 1032–1045.
3 S. Ben-Haim and O. Israel, *Semin. Nucl. Med.*, 2009, **39**, 408–415.
4 K. Strobel, *Praxis*, 2009, **98**, 1293–1297.
5 K. Liepe, J. Kropp, R. Runge and J. Kotzerke, *Br. J. Cancer*, 2003, **89**, 625–629.
6 H. Palmedo, S. Guhlke, H. Bender, J. Sartor, G. Schoeneich, J. Risse, F. Grunwald, F. F. Knapp and H. J. Biersack, *Eur. J. Nucl. Med. Mol. Imaging*, 2000, **27**, 123–130.
7 J. M. H. de Klerk, A. van Dijk, A. D. van het Schip, B. A. Zonnenberg and P. P. van Rijk, *J. Nucl. Med.*, 1992, **33**, 646–651.
8 A. Handeland, M. W. Lindegaard and D. E. Heggli, *Eur. J. Nucl. Med. Mol. Imaging*, 1989, **15**, 609–611.
9 R. T. M. de Rosales, C. Finucane, S. J. Mather and P. J. Blower, *Chem. Commun.*, 2009, 4847–4849.
10 R. T. M. de Rosales, C. Finucane, J. Foster, S. J. Mather and P. J. Blower, *Bioconjugate Chem.*, 2010, **21**, 811–815.
11 K. Verbeke, J. Rozenski, B. Cleynhens, H. Vanbilloen, T. Groot, N. Weyns, G. Bormans and A. Verbruggen, *Bioconjugate Chem.*, 2002, **13**, 16–22.
12 K. Ogawa, T. Mukai, Y. Inoue, M. Ono and H. Saji, *J. Nucl. Med.*, 2006, **47**, 2042–2047.
13 E. Palma, B. L. Oliveira, J. D. G. Correia, L. Gano, L. Maria, I. C. Santos and I. Santos, *JBIC, J. Biol. Inorg. Chem.*, 2007, **12**, 667–679.
14 A. Datta, P. Panwar, K. Chuttani and A. K. Mishra, *Cancer Biol. Ther.*, 2009, **24**, 123–128.
15 G. Shukla, A. K. Tiwari, D. Sinha, R. Srivastava, H. Cahndra and A. K. Mishra, *Cancer Biother. Radiopharm.*, 2009, **24**, 209–214.
16 K. R. Bhushan, P. Misra, F. Liu, S. Mathur, R. E. Lenkinski and J. V. Frangioni, *J. Am. Chem. Soc.*, 2008, **130**, 17648–17649.
17 J. Liu, F. Wang, J. Zhang, S. Yang, H. Guo and X. Wang, *J. Labelled Compd. Radiopharm.*, 2007, **50**, 1243–1247.
18 P. Panwar, S. Singh, N. Kumar, H. Rawat and A. K. Mishra, *Bioorg. Med. Chem.*, 2007, **15**, 1138–1145.
19 A. A. El-Mabhouh, C. A. Angelov, R. Cavell and J. R. Mercer, *Nucl. Med. Biol.*, 2006, **33**, 715–722.
20 D. Kumar, V. Kumar, D. G. Little, R. B. Howman-Giles, E. Wong and S. O. Ali, *J. Orthop. Sci.*, 2006, **11**, 512–520.
21 J. Doubsky, M. Laznicek, A. Laznickova and L. Leseticky, *J. Radioanal. Nucl. Chem.*, 2004, **260**, 53–59.
22 M. Shigematsu, S. Shiomi, H. Iwao and H. Ochi, *Ann. Nucl. Med.*, 2002, **16**, 55–59.
23 R. Alberto, *Top. Curr. Chem.*, 2005, **252**, 1–44.
24 R. Alberto, *Eur. J. Inorg. Chem.*, 2009, 21–31.
25 J. D. G. Correia, A. Paulo and I. Santos, *Curr. Radiopharmaceuticals*, 2009, **2**, 277–294.
26 S. Alves, A. Paulo, J. D. G. Correia, L. Gano, C. J. Smith, T. J. Hoffman and I. Santos, *Bioconjugate Chem.*, 2005, **16**, 438–449.
27 S. Mundwiler, R. Waibel, B. Spingler, S. Kunze and R. Alberto, *Nucl. Med. Biol.*, 2005, **32**, 473–484.
28 R. Alberto, R. Schibli, A. Egli, P. A. Schubiger, W. A. Herrmann, G. Artus, U. Abram and T. A. Kaden, *J. Organomet. Chem.*, 1995, **493**, 119–127.
29 G. R. Kieczykowski, R. B. Jobson, D. G. Melillo, D. F. Reinhold, V. J. Grenda and I. Shinkai, *J. Org. Chem.*, 1995, **60**, 8310–8312.
30 http://www.cyberlipid.org/phlipt/pl2a0006.htm.
31 G. M. Sheldrick, *SADABS*, Bruker AXS Inc., Madison, Wisconsin, USA, 2004.
32 *Bruker. SMART and SAINT*, Bruker AXS Inc., Madison, Wisconsin, USA, 2004.
33 A Altomare, M. C. Burla, M. Camalli, G. L. Cascarano, C. Giacovazzo, A. Guagliardi, A. G. G. Moliterni, G. Polidoro and R. Spagna, *J. Appl. Crystallogr.*, 1999, **32**, 115–119.
34 G. M. Sheldrick, *SHELXL-97: Program for the refinement of crystal structures*, University of Gottingen, Germany, 1997.
35 L. J. Farrugia, *J. Appl. Crystallogr.*, 1999, **32**, 837–838.
36 L. J. Farrugia, *J. Appl. Crystallogr.*, 1997, **30**, 565.
37 F. Marques, K. P. Guerra, L. Gano, J. Costa, M. P. Campello, L. M. Lima, R. Delgado and I. Santos, *JBIC, J. Biol. Inorg. Chem.*, 2004, **9**, 859–872.
38 T. J. Hoffman, W. A. Volkert, D. E. Troutner and R. A. Holmes, *Int. J. Appl. Radiat. Isot.*, 1984, **35**, 223–225.
39 F. Marques, L. Gano, M. P. Campello, S. Lacerda, I. Santos, L. M. Lima, J. Costa, P. Antunes and R. Delgado, *J. Inorg. Biochem.*, 2006, **100**, 270–280.

